2020 IEEE/RSJ International Conference on Intelligent Robots and Systems (IROS)
October 25-29, 2020, Las Vegas, NV, USA (Virtual)

A Neural Primitive model with Sensorimotor Coordination for Dynamic Quadruped Locomotion with Malfunction Compensation

Azhar Aulia Saputra, Auke Jan Ijspeert, and Naoyuki Kubota

Abstract— **In the field of quadruped locomotion, dynamic locomotion behavior, and rich integration with sensory feedback represents a significant development. In this paper, we present an efficient neural model, which includes CPG and its sensorimotor coordination, and demonstrate its implementation in a quadruped robot to show how efficient integration of motor and sensory feedback can generate dynamic behavior and how sensorimotor coordination reconstructs the sensory network for leg malfunction compensation. Additionally, we delineate a network optimization strategy and suggest sensorimotor coordination as a strategy for controlling speed and regulating internal and external adaptation. The rhythm generation representing the leg injury was inactive, stimulating the sensorimotor system to reconstruct the network between CPG and feet force afferent without any commanding parameter. The performances of the simulated and real, cat-like robot on both flat and rough terrains and the leg malfunction tests demonstrated the effectiveness of the proposed model, indicating that a smooth gait-pattern transition could be generated during sudden leg malfunction.**

Index Terms— **Neural-based Locomotion, Sensorimotor Coordination, Malfunction Compensation, Quadruped Robot**

I. Introduction

Locomotive capacity is essential for movement in a dynamic environment; animals exemplify this, having to move efficiently to conduct their activities. Quadruped animals, specifically, produce dynamic locomotion patterns ranging from walking to galloping. These patterns are generated by CPG structures using sensory feedback and spinal reflexes [1]. Primitive CPG structures generate dynamic patterns even when sensory feedback and signal commanding are absent [2]. In the last two decades, integrating neuroscience and robotic locomotion has been considered as an alternative approach to dynamic locomotion. Many researchers have proposed CPG concepts in the service of robot locomotion [3], [4], [5]. However, the question of the best way of controlling quadruped locomotion has yet to be resolved.

Quadruped locomotion based on CPG is a part of various strategies for controlling speed and direction. Some researchers have used mapping selection of the CPG network to generate various gait patterns [6], [7], [8], [9], [10]. Our previous research used a generic locomotion model that enabled the generation of various gaits using simple parameter changes made by selecting designed coupling matrices. Sensory feedback affects the CPGs change-of-the-state pace [8], [11]. Furthermore, we used an optimization model to identify the appropriate CPG structure for the desired gait pattern [12]. Other researchers have also used CPG for pattern generation [13]. In [13], CPG generated a signal to stimulate a certain leg to perform a stepping movement; the stepping pattern had been mapped beforehand. Kimura et al. developed various CPG that were integrated with sensory feedback to generate torque [14] and gait-pattern modulation [9]. However, CPG has been reconstructed as development changes the individual body (e.g., infants to mature, frog) [15]. Generating different gait patterns without abruptly reconstructing the network is still challenging: creating an efficient structure that can generate dynamic patterns and developing integration of sensory feedback to establish swing timing have still not been achieved [5], [16].

In some cases, the spinal cord systems of humans and animals regulate locomotion when a leg is injured, changing the role of sensory feedback within the locomotion network [17], [18]. In the field of robotics, Ren et al. have considered the leg-injury compensation in the hexapod robot using multiple chaotic CPG and a master-client strategy [19]. Some researchers tend to use conventional approaches to solving leg malfunction problems in the legged robots [20]. Still, conventional models need to consider many aspects, leading to a high computational cost, and it has proven difficult to find the correct strategy for compensating a broken leg using CPG in quadrupedal locomotion. Considering the sensorimotor coordination mechanism is important for developing dynamic locomotion in cases of malfunction.

This paper responds to the current challenges facing developing CPG for quadruped locomotion, presenting an efficient, robust CPG model that is dynamically integrated with sensory feedback to generate various gaits while also considering leg malfunction compensation without involving too many parameters. The model uses two sensorimotor-coordinationbased mechanisms [18], [17]: 1) because sensory feedback is critical for adjusting CPG modulation, proprioceptive signals from the leg force and swinging phases are integrated with rhythm-generator neurons (RG) in the CPG; 2) because leg malfunction affects the integration of sensory feedback and RG, a neuron representing a certain injured leg sends a signal and influences the effect of the sensory signal on RG. The proposed models novel contributions follow:

1) Developing a robust CPG model with an efficient structure that can generate various gait patterns.

This work was partially supported by a Grant-in-Aid for Scientific Research (18J21284) from Japan Society for the Promotion of Science.

Azhar Aulia Saputra and Naoyuki Kubota are with the Graduate School of System Design, Tokyo Metropolitan University, 6-6 Asahigaoka, Hino, Tokyo, 191-0065, Japan (e-mail: azhar-aulia-saputra@ed.tmu.ac.jp; kubota@tmu.ac.jp;).

Auke Jan Ijspeert is with Biorobotics Laboratory, Ecole Polytechnique Féderalé de Lausanne, Switzerland (e-mail: auke.ijspeert@epfl.ch).

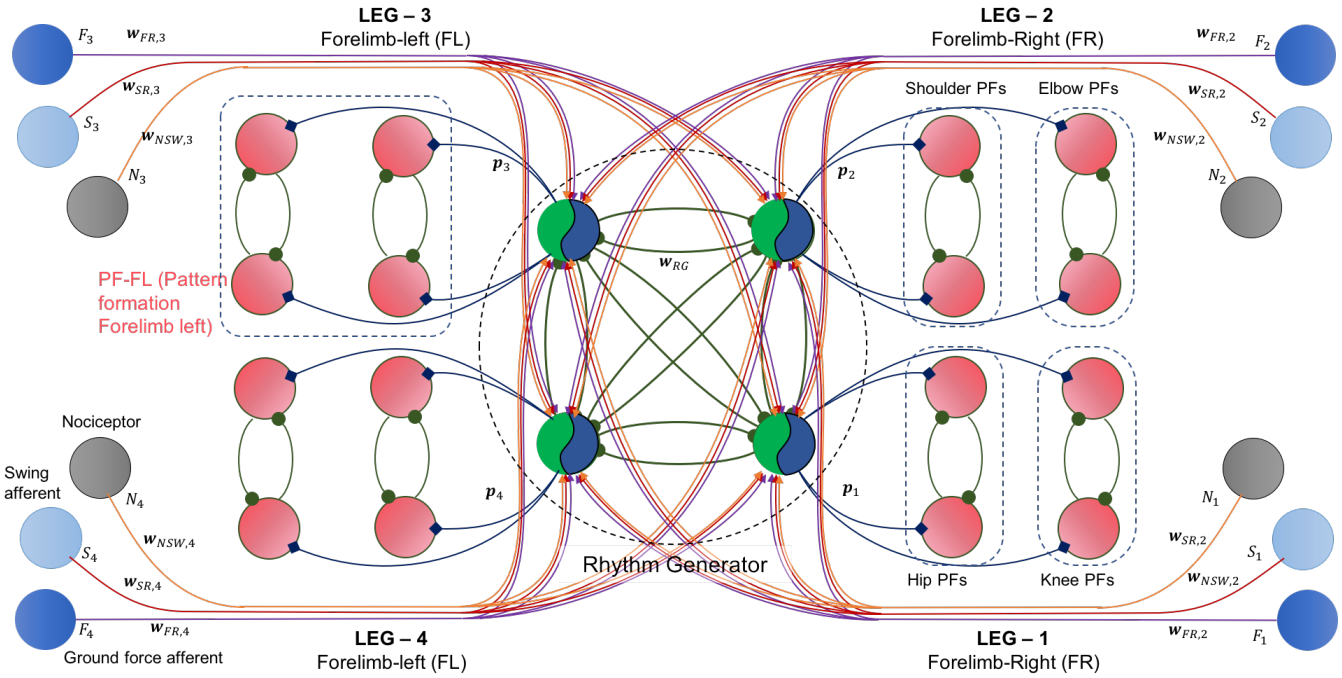

Fig. 1. Design of the single rhythm CPG model with two-layered CPG. Every leg has three sensory-feedback-to-all RG, a force sensor, a pain receptor, and a swing sensor

2) Integrating sensory feedback that substantially impacts the CPG-modulation output.
3) Considering dynamic sensorimotor integration to compensate leg injuries at various speeds.

Furthermore, to demonstrate the proposed models effectiveness, we have used a cat-like robot that performs in various contexts, including in different terrains, at different speeds, and with leg injuries.

This paper is organized as follows: the proposed CPG model with sensorimotor coordination is presented in Section II; the strategy for finding the optimum structure is delineated in Section III; Section IV presents the experimental results; finally, in Section V, we conclude the research and discuss the prospects of the proposed model.

II. CPG with Sensorimotor Coordination

The CPG model dynamically generates locomotion patterns. In cat studies, two-layered CPG has been observed, incorporating rhythm generators (RG) and pattern formation (PF) [21]. We have designed a single-model CPG where one RG represents one legs movement pattern, and one PF neuron represents the activation of one muscle. Since each leg uses four muscles (flexor and extensor muscles of the hip and knee joints), there is one RG neuron and four PF neurons for each CPG structure. Our model uses two CPG pairs; every pair represents the forelimb and hindlimb for another pair. Fig. 1 shows the complete design of the proposed CPG model.

Rhythm-generator neurons generate oscillation signals responsible for controlling the patterns of a certain leg. All of the RG are interconnected and control the timing of the legs swing action. We used the Matsuoka neural-oscillator model to generate a dynamic signal. The inner state of the RG neuron is as follows:

$$\tau \frac{\mathrm{d}}{\mathrm{d}t} x_i = \left(\upsilon_i - x_i - \sum_{j=1}^{n} \mathbf{w}_{RG,ij} y_j + \alpha_i - b v_i \right) (\tau_f * S_{STIM}) \quad (1)$$

The received-inhibition effect of its self-adaptation (v_i) and the signal from other RG neurons (y_j) influenced by synaptic weight (w_{ij}). y_i is calculated as $y_i = \max(x_i, 0)$ and v_i is calculated as follows:

$$T \frac{\mathrm{d}}{\mathrm{d}t} v_i = (y_i - v_i)(\tau_f S_{STIM}) \quad (2)$$

The inner-state and self-adaptation effects are respectively influenced by time constants τ and T. The RG neuron is also influenced by sensory feedback (α_i) from ground-force afferent, swing-related afference, and nociceptors.

$$\alpha_i = \alpha_{i,0} + \sum_{j=1}^{n} (F_i \mathbf{w}_{FR,ij}) + \sum_{j=1}^{n} \left(G_{STIM} S_i (\mathbf{w}_{SR,ij} N_j \mathbf{w}_{NS,ij}) \right) \quad (3)$$

where, $\alpha_{i,0}$ is the basic stimulation of the ith neuron, $\mathbf{w}_{FR,ij}$ and $\mathbf{w}_{SR,ij}$ are the synaptic weights of the force afferent (F_i) and the swing-phase afferent (S_i) of the ith leg to the jth RG neuron. Swing-afferent feedback is influenced by the nociceptor (N_i); its weight is represented by $\mathbf{w}_{NS}$. The nociceptor (N_i) is a pain receptor that detects the condition of leg damage and sends damage stimuli to RG neurons, affecting sensory stimulation from the ground-force afferent to the RG neurons and from the swing-related afferent to the RG neurons. Parameter G_{STIM} is the gain parameter controlling the relationship between speed stimulation S_{STIM} and the sensory network. The gain parameter is assumed to differently affect the forelimbs and hindlimbs. Based on preliminary tests, the G_{STIM} for hindlimbs is calculated as $G_{STIM} = \mu_{HL}/(1+$

$\exp(-\lambda_{HL}S_{STIM}+\eta_{HL}))$ and the G_{STIM} for hindlimbs is calculated as $G_{STIM}=\exp(\log(\mu_{HL})(\lambda_{FL}S_{STIM}-\eta_{FL})^2)$

Given the RG neurons control the movement-pattern phase for each leg, they transmit the firing signal (p_i) to all PF neurons in a certain leg to activate swing behavior. This is calculated as follows:

$$p_i=\begin{cases}1 & \text{if } (y_i+h_i^{ref})\geq\Theta\\ 0 & \text{0therwise}\end{cases} \tag{4}$$

where Θ is the firing threshold. The value of h_i^{ref} is calculated as follows:

$$h_i^{ref}(t)=\begin{cases}\gamma^{ref}\cdot h_i^{ref}(t-1)-R & \text{if } p_i(t-1)=1\\ \gamma^{ref}\cdot h_i^{ref}(t-1) & \text{otherwise}\end{cases} \tag{5}$$

When the RG signal is fired, R is subtracted from the $h_i^{ref}(t)$ value of neuron i. $R>0$, ^{ref} is a discount rate of h_i^{ref}, and $0\gamma^{ref}1$. The firing value of the ith RG neuron $p_i(t)$ is generated for all PF neurons in the ith leg.

Upon receiving the firing signal from RG neurons (p_i), PF neurons perform the swing behavior by activating muscle stimulation explained in [22]. The PF neurons control the timing of each muscle contraction. The activation signal generated by PF neurons is calculated as follows: (To control the speed, speed stimulation is adjusted from parameter S_{STIM}, which influence Eqs. (1) and (3))

$$\theta_{i,k}(t)=e^{\left(\log(0.5)\times\left(\frac{|PF_i-\mu|}{(\mu\times w)}^3\right)\right)} \tag{6}$$

where, PF_i neurons are calculated as $PF_i(t)=PF_i(t-1)+p_i$, d_{Opt} represents the starting control, calculated by $\mu=(30-\phi_i^{(LEG})/30$, w represents the time of the activation signal, calculated as $w=\psi_i^{(LEG}/50$. $\phi_i^{(LEG}$, and $\psi_i^{(LEG}$ is the parameter for controlling swing activation and the timing of the ith PF neuron in certain LEG; F for forelimb and H for hindlimb. The values of ϕ and ψ were optimized in our previous research using a multi-objective evolutionary algorithm.

III. Optimization Strategy

To find the best CPG structure, we optimized the weights representing the interconnection of RG neurons ($\mathbf{w}_{RG}$) and those representing interconnection with sensory feedback ($\mathbf{w}_{FR}$, $\mathbf{w}_{SR}$, $\mathbf{w}_{NS}$) using a single-objective evolutionary algorithm (SOEA). There were two optimization steps: 1) building a dynamic gait pattern; 2) building a malfunction compensator.

A. Dynamic Gait Pattern Optimization

This optimization aims to identify the best interconnection of RG neurons, and integration with sensory feedback, for generating dynamic gait patterns without changing the interconnection structure. We optimized a matrix parameter, representing the interconnection of RG neurons ($\mathbf{w}_{FR}$), the connection between force sensory feedback and RG neurons $\mathbf{w}_{SR}$, and the swing-phase-to-RG-neuron feedback ($\mathbf{w}_{NS}$). Those parameters are represented by 23 parameters

TABLE I

Representation of optimized parameter

		RG Neuron ID			
	$\mathbf{w}_{RG}$	1	A	B	C
RG Neuron ID	1	0	r_2	r_3	r_4
	A	r_5	0	r_6	r_7
	B	r_3	r_4	0	r_2
	C	r_6	r_7	r_5	0

	Leg			
$\mathbf{w}_{FR}$	1	2	3	4
1	r_8	r_{12}	r_{12}	r_8
2	r_9	r_{13}	r_{13}	r_9
3	r_{10}	r_{14}	r_{14}	r_{10}
4	r_{11}	r_{15}	r_{15}	r_{11}

	Leg			
$\mathbf{w}_{NS}$	1	2	3	4
1	r_{16}	r_{20}	r_{20}	r_{16}
2	r_{17}	r_{21}	r_{21}	r_{17}
3	r_{18}	r_{22}	r_{22}	r_{18}
4	r_{19}	r_{23}	r_{23}	r_{19}

r_1	1	2	3	4	5	6
A	1	1	2	2	3	3
B	2	3	3	1	1	2
C	3	2	1	3	2	1

($r_1, r_2, r_3, \cdots, r_23$) optimized using SOEA; Table 1 shows a detailed representation of the parameter I. The value of A, B, and C identify the RG neurons calculated from parameter r_1.

We minimized errors of speed oscillation, desired speed, and speed stimulation. For each evaluation process, we performed the robot simulation six times at different speed stimulations compared to parameters τ_f in Eq. (1); each performance required 1000 time cycle processes. We recorded the distance achieved (d_i) by each performance. The evaluation function is as follows:

$$f=\sum_{i=1}^{5}\left(\frac{1}{1+\exp(d_i-d_{i+1})}\right)+\frac{1}{T}\sum_{t=1}^{T}\sqrt{(\alpha(t))^2} \tag{7}$$

where, T is the number of time steps, defined as 1000, and $\alpha(t)$ is the torso acceleration for time step t.

B. Malfunction Compensation Optimization

After optimizing the dynamic gait pattern, we optimized the connection between nociceptor and RG neurons ($\mathbf{w}_{NS}$). For this optimization, we found the best motion pattern was the leg malfunction condition. We used the optimized $\mathbf{w}_{RG}$, $\mathbf{w}_{SR}$, and $\mathbf{w}_{FR}$. We assume that the nociceptor may stimulate each RG neurons with a different effect. There were 16 parameters: ($\mathbf{w}_{NS,1-1}, \mathbf{w}_{NS,1-2}, \cdots, \mathbf{w}_{NS,4-4},$).

To evaluate each set of parameters, we performed the simulation four times with different leg injuries. Under normal conditions, the value of N_i was zero ($N=\{0,0,0,0\}$). When the ith leg was injured, the value of N_i was one ($N_i=1$). There were four steps, where $N_{STEP}=1$. For every step, we evaluated the performance of the robot as follows:

$$f_{STEP}=\frac{1}{1+\exp(-d_{STEP}^{SAG})}+\sqrt{(d_{STEP}^{FRO})^2} \tag{8}$$

where f_{STEP} is the fitness function of a particular step-malfunction performance and d_{STEP}^{SAG} and d_{STEP}^{FRO} are the distance of the robot's movement in the sagittal and frontal directions. This optimization forces the robot to move straight ahead with minimal frontal direction movement.

IV. Experimental Result

This experiment shows the results of the optimization processes of dynamic gait pattern and malfunction compensator in a computer simulation using an Open Dynamics Engine (ODE). Following this, we demonstrated the dynamic

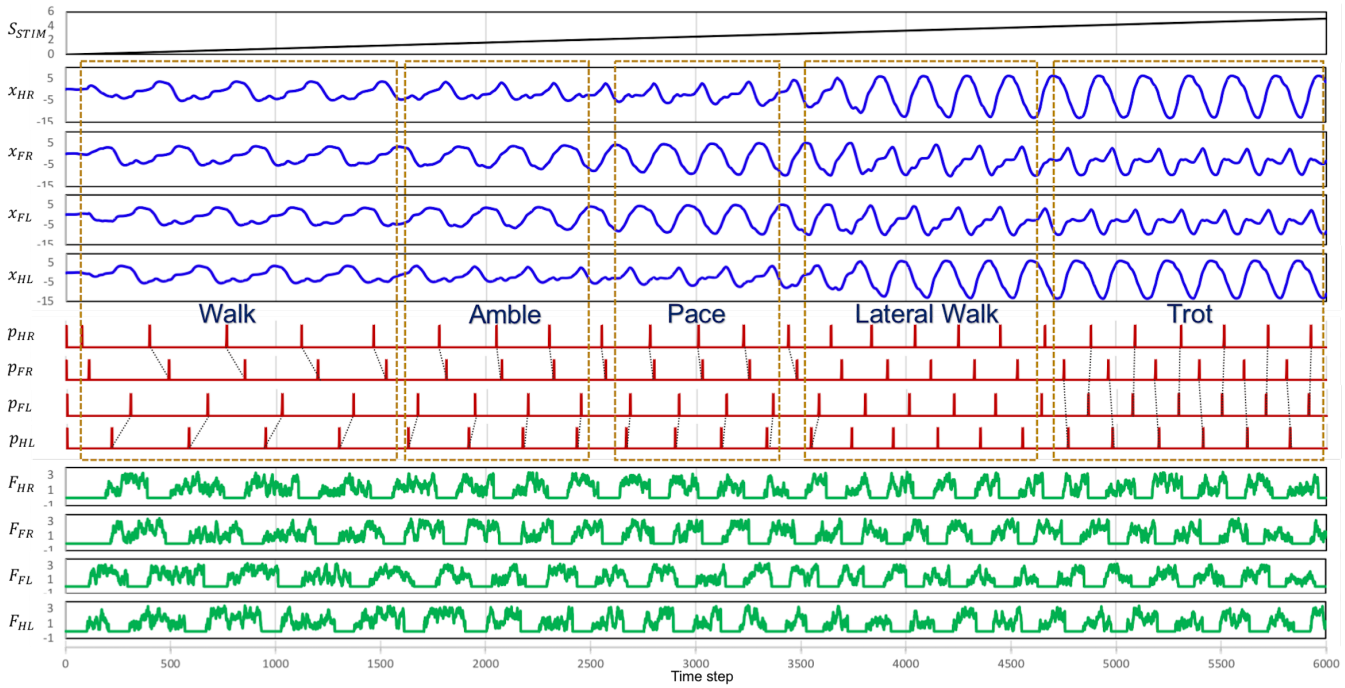

Fig. 2. The CPG model can generate a dynamic gait pattern through differing speed stimulation S_{STIM}. This increases the frequency of the CPG outputs $\mathbf{x}$ of five different known gait patterns from slow speed to high speed. Parameter F_{HR}, F_{FR}, F_{HL}, F_{FL} shows the ground reaction force for every limb.

TABLE II

THE VALUE OF DEFINED PATTERN FORMATION PARAMETERS FROM PRELIMINARY TEST

	val.		val.		val.		val.
$\phi_1^{(F)}$	0.034	$\phi_2^{(F)}$	12	$\phi_3^{(F)}$	12	$\phi_4^{(F)}$	0.034
$\phi_1^{(H)}$	13	$\phi_2^{(H)}$	0.012	$\phi_3^{(H)}$	0.012	$\phi_4^{(H)}$	13
$\psi_1^{(F)}$	20	$\psi_2^{(F)}$	10	$\psi_3^{(F)}$	10	$\psi_4^{(F)}$	20
$\psi_1^{(H)}$	0.034	$\psi_2^{(H)}$	0.013	$\psi_3^{(H)}$	0.012	$\psi_4^{(H)}$	0.034
μ_{HL}	1.676	μ_{FL}	0.501	T	1 .0	λ_{FL}	2.04
b	1.5	τ_f	1.2	R	12.5	$\alpha_{i,0}$	3.45

movement of the robot in the contexts of simulation and real robot implementation. For the robot simulation, we used a cat-like robot with an implemented muscle-based actuator model. The robots size was adjusted according to a cats size. We have defined the parameters not optimized in Table II

A. Optimization of Dynamic Gait Pattern

This optimization process used SSGA, which features 128 individuals in every population, and we optimized until the 200 generation. This optimization performance was validated to optimize neural interconnection [23]. Fig. 3 shows the results, indicating the fitness value decreasing gradually. The signal response to the gait pattern was evaluated using different speed stimulations. We performed the robot simulation in 6000 time steps (30 seconds). Fig.4, is a snapshot of the robots performance; more robot performance documentation is supplied in the supplementary video. We set S_{STIM} from zero and gradually increased it with the value of the time step ($S_{STIM} =$ time step$/1200$); the result are presented in Fig. 2. The CPG model can generate dynamic gait patterns from five known gait patterns. These range from slow to high speeds: walk; amble; pace; symmetrical walk; trot. However, the symmetrical-walk pattern between pace and trot gaits does

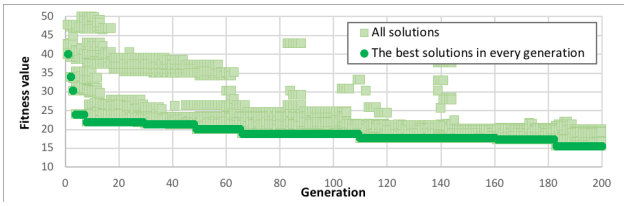

Fig. 3. The graph shows the evolution of the fitness value of gait pattern

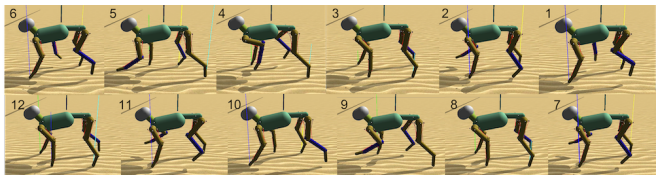

Fig. 4. The sample result in Open Dynamic Engines

not exist in animal locomotion. However, in the proposed model, the symmetrical walk gait makes the transition from pace to trot.

Furthermore, to demonstrate the sensory aspect of gait-pattern generation, we tested the robot in rough terrain and evaluated the RG signal. We set the S_{STIM} at 0.5 so that the robot would generate the walking gait normally; Fig. 5 shows the results. During movement on rough terrain, swing time changed depending on contact time. Force feedback, or the end of swing time, influenced the RG as well as the gait pattern.

B. Optimization of Malfunction Compensation

This optimization used the best parameters from the previous optimization. There were 64 individuals in each population. We optimized up to 200 generations; that is,

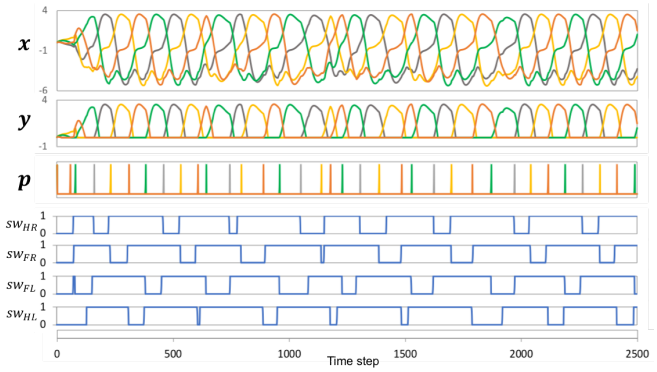

Fig. 5. The effect of sensory feedback in the RG during movement on rough terrain. sw_{HL} is the swing phase condition of the left hindlimb. **x** is the output signals of CPG calculated by Eq. 1. By analyzing the signal pattern **p**, we can see the pattern is changing to respond to the different force feedback or swing phase.

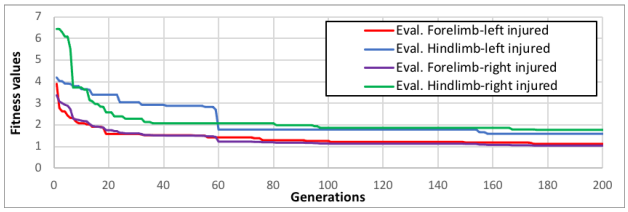

Fig. 6. The graph shows the evolution of the fitness value for malfunction compensation

12800 evaluations. A similar evaluation was performed for different leg injury conditions. The fitness functions results are shown in Fig. 6 shows the results for this evaluation, indicating that four fitness values were decreasing. The best fitness value was achieved for the hindlimb condition.

To evaluate the optimized parameters effectiveness, we performed the simulation in normal conditions and then disabled one of the forelimbs or hindlimbs through injury. We also gradually changed the speed stimulation (S_{STIM}) to evaluate the gait-pattern response during leg injury. Fig. 7 shows the results, indicating that the proposed CPG model can respond to the leg injury signal through a smooth transition to both forelimb and hindlimb leg injury. There are different gait patterns under leg injury conditions. The model changed the gait pattern by controlling the signal input using sensory feedback. During leg injury, the model can still generate dynamic gait patterns by stimulating a different speed.

C. Real Robot Implementation

To demonstrate the effectiveness of the proposed model, we implemented the proposed model in the cat-like robot AQuRo-v3. The robot is rendered in Fig. 8. The robot is made from 3D printed material and features 21 degrees of freedom (5 degrees of freedom for each of the 4 legs, and 1 degree of freedom for the neck) actuated by a servo motor. The robot used a NUC PC core i5 with four force sensors (one sensor for one leg), an inertial measurement unit (IMU), and four time-of-flight sensors.

The robots gait pattern has been controlled by the proposed

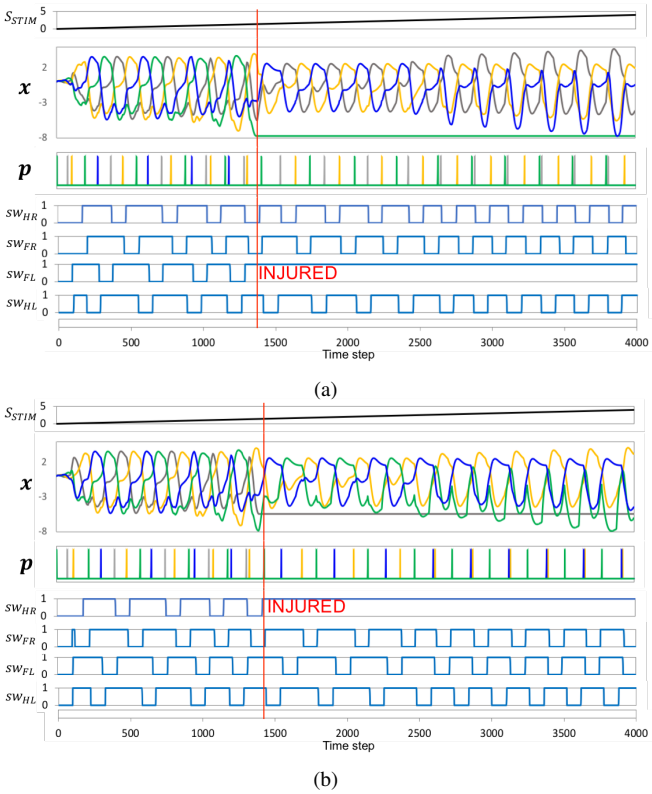

Fig. 7. The generated gait patterns in malfunction conditions and the speed stimulation responses. The signal pattern (**p**) is changing to respond to the absence of CPG signals. The time phase decreases after a leg is injured. a) malfunction of the right forelimb at time step 1380. During injury, the model tends to generate a pattern with the same phase difference at a lower speed. At high speeds, left and right hindlimbs feature the same phase. b) malfunction of the left hindlimb at time step 1400. In this condition, the left and right forelimbs feature the same phase at a higher speed.

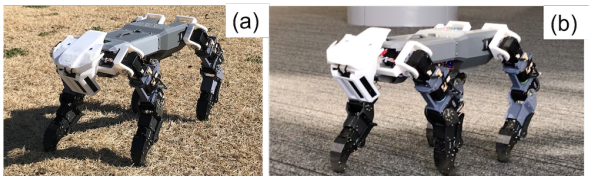

Fig. 8. The appearance of the robot

CPG model. We used similar parameters for the simulation performance. First, we operated the robot with different speed stimulations on different terrains. The robot was able to move on both terrains with a dynamic gait pattern. There is a supplementary video of the robots performance, while Fig. 9 shows a sample snapshot. The robot was able to generate four gaits: walk, amble, pace, and trot.

Furthermore, we demonstrated the effectiveness of malfunction compensation by conducting tests in two conditions: injured forelimb and injured hindlimb. In these tests, the robot first moves normally. Then, after a few seconds, one of the legs was set to injured. The robot could generate a gait transition without falling in both conditions. We operated the robot on both flat and natural terrain. Fig. 10 is a snapshot of the robots performance; more detail is shown in the supplementary video provided or otherwise located at `https://youtu.be/C_XEsahqjpA`.

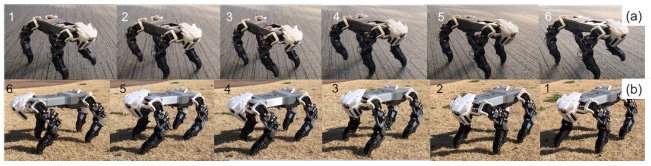

Fig. 9. Snapshots of the robot performance show the dynamic gait pattern: a) the robots performance on flat terrain; b) the robots performance on natural terrain.

Fig. 10. Snapshots of the robots performance shows the dynamic gait pattern during leg injury: a) the robots performance on the flat terrain with a forelimb injury; b) the robots performance on flat terrain with a hindlimb injury; c) the robots performance on natural terrain with a forelimb injury; d) the robots performance on natural terrain with a hindlimb injury.

V. Conclusion and Discussion

This paper has presented an efficient dynamic-gait-pattern-generationbased CPG mechanism with sensorimotor coordination. The model developed features substantial integration of CPG and sensory feedback, indicating that sensory feedback has a role in gait-pattern generation. The CPG structure uses a two-layer CPG model comprising a single RG and PF pools. Each leg is represented by a single CPG. Four RGs represent the four limbs. There are three sensory neurons in every leg: force sensor, swing phase, and pain receptor neurons. Section II explained the assumption of the integration of sensory neurons and RG neurons. However, it required optimization to achieve the best integration.

We used SOEA to optimize the network, a process separated into two steps: 1) gait pattern optimization; 2) malfunction compensation. There were two steps to optimizing integration and structure under normal conditions before manipulating the malfunction problem, enabling the model to generate a dynamic gait pattern through stimulation from only a single parameter (S_{STIM}). There are five patterns generated by robot performance: walk, amble, pace, symmetrical walk, and trot gait. Force feedback also has a big influence on generating gait pattern; this was demonstrated by the robots performance on rough terrain (see Fig. 5). The RG signal changed dynamically with changes to sensory input, and the proposed model generated gait transition between normal and injured conditions. It was also shown to generate dynamic gait during leg injuries.

In the real implementation, a cat-like quadruped robot demonstrated the effectiveness of the proposed model on steep terrain. Actuator control levels differed between the real robot and the simulation. However, these were controlled by the same gait pattern and did not impact the effectiveness of the proposed CPG model.

In future work, the proposed model should be applied to more challenging behavior, such as transitioning from ground movement to water movement. For this next step, understanding the role of sensory feedback for cat or dog water movements would be critical.

References

[1] K. Pearson *et al.*, "Assessing sensory function in locomotor systems using neuro-mechanical simulations," *Trends in neurosciences*, vol. 29, no. 11, pp. 625–631, 2006.

[2] Orlovskiĭ, *Neuronal control of locomotion: from mollusc to man*.

[3] J. Yu *et al.*, "A survey on cpg-inspired control models and system implementation," *IEEE transactions on neural networks and learning systems*, vol. 25, no. 3, pp. 441–456, 2013.

[4] A. A. Saputra *et al.*, "Evolving a sensory-motor interconnection for dynamic quadruped robot locomotion behavior," in *Proc. of Intl. Conf. on Intelligent Robots and Systems (IROS)*, 2018, pp. 7089–7095.

[5] A. J. Ijspeert, "Central pattern generators for locomotion control in animals and robots: a review," 2008.

[6] C. P. Santos and V. Matos, "Gait transition and modulation in a quadruped robot: A brainstem-like modulation approach," *Robotics and Autonomous Systems*, vol. 59, no. 9, pp. 620–634, 2011.

[7] C. Liu *et al.*, "Cpg driven locomotion control of quadruped robot," in *Intl. Conf. on Systems, Man and Cyb.*, 2009, pp. 2368–2373.

[8] L. Righetti and A. J. Ijspeert, "Pattern generators with sensory feedback for the control of quadruped locomotion," in *Intl. Conf. on Robotics and Auton.*, 2008, pp. 819–824.

[9] Y. Fukuoka and H. Kimura, "Dynamic locomotion of a biomorphic quadruped tekkenrobot using various gaits: walk, trot, free-gait and bound," *Applied Bionics and Biomec.*, vol. 6, no. 1, pp. 63–71, 2009.

[10] J. Zhang *et al.*, "Trot gait design and cpg method for a quadruped robot," *Journal of Bionic Engineering*, vol. 11, no. 1, pp. 18–25, 2014.

[11] A. A. Saputra *et al.*, "Biologically inspired control system for 3-D locomotion of a humanoid biped robot," *IEEE Tran. on Systems, Man, and Cybernetics: Systems*, vol. 46, no. 7, pp. 898–911, 2016.

[12] A. A. Saputra and N. Kubota, "Synthesis of neural oscillator based dynamic rhythmic generation in quadruped robot locomotion," in *Proc. of Intl. Elec. Symp. on Knowledge Creation and Intell. Comp. (IES-KCIC)*, 2018, pp. 184–191.

[13] C. Liu *et al.*, "Adaptive walking control of quadruped robots based on central pattern generator (cpg) and reflex," *Journal of Control Theory and Applications*, vol. 11, no. 3, pp. 386–392, 2013.

[14] H. Kimura, S. Akiyama, and K. Sakurama, "Realization of dynamic walking and running of the quadruped using neural oscillator," *Autonomous robots*, vol. 7, no. 3, pp. 247–258, 1999.

[15] H. Ten Donkelaar, "Evolution of vertebrate motor systems," *Brain evolution and cognition*, pp. 77–112, 2001.

[16] K. G. Pearson, "Generating the walking gait: role of sensory feedback," in *Prog. in brain rsrch.* Elsevier, 2004, vol. 143, pp. 123–129.

[17] T. Lam and K. G. Pearson, "The role of proprioceptive feedback in the regulation and adaptation of locomotor activity," in *Sensorimotor Control of Movement and Posture*. Springer, 2002, pp. 343–355.

[18] S. Rossignol and A. Frigon, "Recovery of locomotion after spinal cord injury: some facts and mechanisms," *Annual review of neuroscience*, vol. 34, pp. 413–440, 2011.

[19] G. Ren *et al.*, "Multiple chaotic central pattern generators for locomotion generation and leg damage compensation in a hexapod robot," in *IEEE Intl. Conf. on Intell. Robots and Systems*, 2012, pp. 2756–2761.

[20] Y.-J. Lee and S. Hirose, "Three-legged walking for fault-tolerant locomotion of demining quadruped robots," *Advanced Robotics*, vol. 16, no. 5, pp. 415–426, 2002.

[21] I. A. Rybak *et al.*, "Modelling spinal circuitry involved in locomotor pattern generation: insights from the effects of afferent stimulation," *The Journal of physiology*, vol. 577, no. 2, pp. 641–658, 2006.

[22] A. A. Saputra *et al.*, "A muscle-reflex model of forelimb and hindlimb of felidae family of animal with dynamic pattern formation stimuli," in *Proc of 2020 Intl. Joint Comf. on Neural Networks*, July 2020.

[23] A. A. Saputra *et al.*, "Interconnection structure optimization for neural oscillator based biped robot locomotion," in *IEEE Symp. Series on Comp. Intell.*, 2015, pp. 288–294.